Insect Systematics and Diversity, (2018) 2(5): 3; 1–14
doi: 10.1093/isd/ixy013
Research

Evolution

Paleotropical Diversification Dominates the Evolution of the Hyperdiverse Ant Tribe Crematogastrini (Hymenoptera: Formicidae)

Bonnie B. Blaimer,[1,5] Philip S. Ward,[2] Ted R. Schultz,[3] Brian L. Fisher,[4] and Seán G. Brady[3]

[1]Department of Entomology and Plant Pathology, North Carolina State University, 100 Derieux Place, Raleigh, NC 27695, [2]Department of Entomology and Nematology, University of California-Davis, Davis, CA 95616, [3]Department of Entomology, National Museum of Natural History, Smithsonian Institution, Washington, DC 20560, [4]Department of Entomology, California Academy of Sciences, San Francisco, CA 94118, and [5]Corresponding author, e-mail: bonnie_blaimer@ncsu.edu

Subject Editor: Marko Mutanen

Received 8 June 2018; Editorial decision 16 August 2018

Abstract

Levels of diversity vary strikingly among different phylogenetic lineages of ants. Rapid radiations in early ant evolution have often proven difficult to resolve with traditional Sanger-sequencing data sets of modest size. We provide a phylogenomic perspective on the evolution of the hyperdiverse ant tribe Crematogastrini by analyzing sequence data for nearly 1,800 ultraconserved element (UCE) loci from 153 species comprising 56 genera. We reconstruct a next-to-complete genus-level phylogeny using concatenated maximum likelihood and species-tree approaches, estimate divergence dates and diversification rates for the tribe, and investigate the evolution of nest sites. Our results show 10 well-supported major clades which we define as the *Cataulacus*, *Carebara*, *Vollenhovia*, *Podomyrma*, *Crematogaster*, *Mayriella*, *Lordomyrma*, *Myrmecina*, *Paratopula*, and *Formicoxenus* genus-groups. These lineages are estimated to have arisen from a Paleotropical ancestor (crown-group age ~75 Ma) over a relatively short time interval (50–70 Ma). The Afrotropical and especially the Indomalayan regions appear to have played a key role in the early diversification history of the tribe. Several shifts in diversification rates were found to be related to the evolution of large, widespread genera; however, we were unable to confidently associate these shifts with evolutionary innovations or events. Arboreal habitats have been successfully colonized by only few clades within Crematogastrini from ground-nesting ancestors, with no reversals supported. Our genus-level phylogeny for Crematogastrini provides insights into the diversification and evolution of one of the most diverse clades of ants, and our division of the tribe into well-supported genus-group lineages sets the stage for more detailed species-level investigations.

Key words: phylogenomics, Myrmicinae, radiation, biogeography, ultraconserved element

An intriguing feature of organismal diversity is the frequent occurrence of related lineages that differ strikingly in species richness and morphological innovation. Such disparities in taxonomic and phenotypic diversification occur at all levels in the tree of life. Classic metazoan examples include bilaterians and nonbilaterians (Dunn et al. 2014); neognath versus paleognath birds (Jarvis et al. 2014, Prum et al. 2015); and pterygote insects and their wingless relatives (Misof et al. 2014). Among the aculeate or stinging Hymenoptera, the ants (Formicidae) are an especially diverse and successful group, as reflected in their high species numbers and varied morphologies and social behaviors in comparison to other aculeates (Gauld and Bolton 1988, Wilson and Hölldobler 1990, Lach et al. 2010). Yet this diversity is far from evenly apportioned among the major lineages of ants (Ward 2014). Thus, there are approximately 13,370 described species of extant ants, distributed among 17 subfamilies (AntCat 2018), yet half of this species diversity resides in just one subfamily, the hyperdiverse Myrmicinae. These ants collectively occupy most terrestrial habitats and exhibit wide variation in ecology, behavior, and colony structure (Kugler 1979, Wilson and Hölldobler 1990, Brown 2000, Anderson et al. 2008, Buschinger 2009). Moreover, the number of described species of Myrmicinae—currently about 6,630—can be expected to grow with greater taxonomic scrutiny.

Recent molecular phylogenetic studies support the division of the Myrmicinae into six mutually exclusive tribes (Ward et al. 2015, Branstetter et al. 2017a), and they too are of uneven size. About 40% of all myrmicine species (and 45% of all myrmicine genera) belong

to the tribe Crematogastrini. This clade appears to have undergone a pronounced radiation after its origin in the late Cretaceous (Ward et al. 2015). Unraveling the details of that history is challenging, however, because numerous old divergences occur close together in time. A data set based on Sanger sequencing of 11 nuclear genes from 100 crematogastrine species (part of a larger study of the subfamily Myrmicinae) produced a poorly resolved 'bush' at the base of the clade (Ward et al. 2015), highlighting the need for more comprehensive gene and taxon sampling.

Here we employ phylogenomic methodology to probe the evolutionary history of crematogastrine ants. Compared to conventional Sanger sequencing, genomic approaches have yielded better resolved trees for ants (Blaimer et al. 2015) and provide an opportunity to refine data matrices and better approximate model assumptions used in phylogenetic inference (Branstetter et al. 2017a). Owing to the still-prohibitive costs of whole-genome sequencing, systematists have gravitated toward several genome-reduction techniques (Lemmon and Lemmon 2013), of which targeted enrichment of ultraconserved elements or UCEs (Faircloth et al. 2012) has proven especially effective for illuminating relationships among ants and other Hymenoptera (Blaimer et al. 2015, 2016b; Branstetter et al. 2017b,c; Ješovnik et al. 2017; Prebus 2017; Ward and Branstetter 2017). In this study, we sequenced a comprehensive sample of crematogastrine species using a new ant-customized UCE probe set that targets 2,590 loci (Branstetter et al. 2017a). Our goals were 1) to generate a robust, time-calibrated phylogeny of the Crematogastrini, 2) to reconstruct biogeographic history and nest-site evolution, and 3) to determine if there were significant shifts in diversification rates among crematogastrine lineages. The results provide a detailed window into the evolution of this highly successful ant clade.

Materials and Methods

Taxon Sampling

We selected 153 ingroup species belonging to 56 crematogastrine genera for our molecular study. These included the 100 Crematogastrini species used in Ward et al. (2015); in all but one case the remaining DNA extracts from that study were used. Fifty-three new taxa were added to achieve a nearly complete sampling of the 64 genera of the tribe. All but four described genera (*Formosimyrma* Terayama, *Goaligongidris* Xu, *Peronomyrmex* Viehmeyer, *Secostruma* Bolton) are included in the present analysis. We further increased our taxon sampling at the species level within some genera to mitigate long branches resulting from single-species representation in the previous study of the subfamily (Ward et al. 2015). Eight outgroup taxa were included: five species representing members of other tribes of the subfamily Myrmicinae (*Manica bradleyi* Wheeler, *Pogonomyrmex imberbiculus* Wheeler, *Aphaenogaster swammerdami* Forel, *Monomorium hanneli* Forel, *Pheidole longispinosa* Forel), as well as members of three other closely related subfamilies (Ectatomminae: *Rhytidoponera chalybaea* Emery, Heteroponerinae: *Acanthoponera minor* Forel, Formicinae: *Formica moki* Wheeler). Supp Table 1 (online only) contains voucher information for all taxa and further specimen data are available on AntWeb (www.antweb.org). Voucher specimens have been deposited at the University of California, Davis; at the National Museum of Natural History, Smithsonian Institution; at the California Academy of Sciences; and at the North Carolina State University Insect Museum. Specimens included in this study were collected in accordance with local regulations and all necessary permits were obtained.

UCE Data Collection

We extracted DNA destructively or nondestructively (specimen retained after extraction) from worker ants or pupae using the DNeasy Blood and Tissue Kit (Qiagen, Valencia, CA). We quantified genomic DNA for each sample using a Qubit fluorometer (High sensitivity kit, Life Technologies, Inc., Carlsbad, CA) and sheared between <5 and 300 ng for 10–60 s (amp = 25, pulse = 10) to a target size of approximately 500–600 bp by sonication (Q800, Qsonica Inc., Newtown, CT). This sheared DNA was used as the input for a modified genomic DNA library preparation protocol (Kapa Hyper Prep Library Kit, Kapa Biosystems, Wilmington, MA) that incorporated 'with-bead' cleanup steps (Fisher et al. 2011) and a generic SPRI substitute (Rohland and Reich 2012, 'speedbeads' hereafter), as described by Faircloth et al. (2015). We used TruSeq-style adapters during adapter ligation (Faircloth and Glenn 2012) and combined groups of 9–10 libraries at equimolar ratios into enrichment pools having final concentrations of 84.7–160 ng/µl. We enriched each pool using a set of custom-designed probes (MYcroarray, Inc., now ArborBiosciences, Ann Arbor, MI) targeting 2,590 UCE loci in ants (Branstetter et al. 2017a). We followed target enrichment procedures for the MYcroarray MYBaits kit (Blumenstiel et al. 2010) except we used a 0.2× concentration of the standard MYBaits concentration and added 0.7 µl of 500 µM custom blocking oligos designed against our custom sequence tags. We ran the hybridization reaction for 24 h at 65°C, subsequently bound all pools to streptavidin beads (Dynabeads MyOne Streptavidin T1, Life Technologies, Inc., Carlsbad, CA) and washed bound libraries according to a standard target capture protocol (Blumenstiel et al. 2010). We used the with-bead approach for PCR recovery of enriched libraries as described in Faircloth et al. (2015). We performed qPCR library quantification and combined libraries at equimolar concentrations into two final pools based on the estimated size-adjusted concentrations. We size-selected these final pools for 250–800 bp with a BluePippin (SageScience, Beverly, MA). For a more detailed description of library and enrichment protocols refer to Blaimer et al. (2016a,b). All of the UCE laboratory work was conducted in and with support of the Laboratories of Analytical Biology (L.A.B.) facilities of the National Museum of Natural History. The pooled libraries were sequenced using two lanes of a 125-bp paired-end Illumina HiSeq 2500 run at the University of Utah's Huntsman Cancer Institute. Quality-trimmed sequence reads generated as part of this study are available from the NCBI Sequence Read Archive under accession SRP149549; trinity assembled contig files are deposited in the Dryad data repository, together with data matrices and tree files (doi:10.5061/dryad.121b453).

Processing and alignment of UCE data

We trimmed the demultiplexed FASTQ data output for adapter contamination and low-quality bases using Illumiprocessor (Faircloth 2013; http://dx.doi.org/10.6079/J9ILL), based on the package Trimmomatic (Bolger et al. 2014). All further data processing described in the following relied on scripts within the PHYLUCE package (Faircloth 2016). We computed summary statistics on the data using the *phyluce_assembly_get_fastq_stats.py* script, and assembled the cleaned reads using the *phyluce_assembly_assemblo_trinity.py* wrapper around the program Trinity (version trinityrnaseq_r20140717) (Grabherr et al. 2011). Average sequencing coverage and contig length across assembled contigs were calculated using *phyluce_assembly_get_trinity_coverage.py*.

Species-specific contig assemblies were aligned to a FASTA file of all enrichment baits using *phyluce_assembly_match_contigs_to_probes.py* (min_coverage = 50, min_identity = 80), creating a relational database containing the matched probes. We used *phyluce_assembly_get_match_counts.py* to generate a list of UCE loci shared across all taxa. Sequence coverage statistics (avg, min,

max) for contigs containing UCE loci were calculated using *phyluce_assembly_get_trinity_coverage_for_uce_loci.py*. The list of UCE loci was then used in the *phyluce_assembly_get_fastas_from_match_counts.py* script to create separate FASTA files for each UCE locus containing sequence data for taxa present at that particular locus. We aligned the sequence data in each of these FASTA files using MAFFT (Katoh et al. 2009) through *phyluce_assembly_seqcap_align.py* (min-length = 20, no-trim). We trimmed our alignment using a wrapper script (*phyluce_assembly_get_gblocks_trimmed_alignment_from _untrimmed.py*) for Gblocks (Castresana 2000) using the following settings: b1 = 0.5, b2 = 0.5, b3 = 12, b4 = 7. We selected a 90% complete matrix (containing loci with alignment data from at least 145 of 161 taxa and retaining 1,763 loci) using the script *phyluce_align_get_only_loci_with_min_taxa.py* and added missing data designators to each file with *phyluce_align_add_missing_data_designators.py*. For concatenated phylogenetic analyses, we combined individual alignments of UCE loci into one nexus alignment file with *phyluce_align_format_nexus_files_for_raxml.py* for subsequent phylogenetic analyses.

Phylogenetic Inference

Analyses using a concatenated data set

We used the program AMAS (Borowiec 2016) to calculate several alignment statistics, e.g., alignment length, amount of missing data, and number of parsimony-informative sites. We also calculated guanine-cytosine (GC) content and GC heterogeneity scores across taxa, as both these variables can bias phylogenetic inference (Bossert et al. 2017). We partitioned the data by individual UCE loci, the preferred approach at the time of analysis (cf. Tagliacollo and Lanfear 2018). We also attempted to select a partitioning scheme from the by-locus character sets with PartitionFinder2 using the *r cluster* algorithm (Frandsen et al. 2015, Lanfear et al. 2017). However, this procedure barely reduced the number of partitions (reduced to 1,691 vs 1,763 loci) and we therefore did not proceed with phylogenetic analysis based on those results. We analyzed the concatenated data matrix of 1,763 partitions, as well as an unpartitioned version of the same with maximum likelihood (ML) best-tree and bootstrap searches (N = 100) in RAxML v8.2.7 (Stamatakis 2014). Given their position and relatively long branch lengths in the above analyses, we investigated the possibility of long-branch attraction (LBA) acting upon three genera: *Rostromyrmex* Rosciszewski, *Cardiocondyla* Emery, and *Ocymyrmex* Emery. We therefore excluded 1) *Rostromyrmex*, 2) *Cardiocondyla*, 3) *Ocymyrmex*, and 4) *Cardiocondyla* and *Ocymyrmex* from the data set and re-ran the analyses for each of these four exclusion sets.

Estimation of gene trees and species tree

We reconstructed gene trees for the 1,763 UCE loci by performing RAxML analyses (best tree and 200 bootstraps) on the individual loci, and then performed weighted statistical binning following Bayzid et al. (2015). This approach examines bootstrap-supported gene trees estimated for every locus and sorts these loci into bins, each of which contains loci with gene trees that do not contain significantly conflicting branches (Mirarab et al. 2014). We used a bootstrap support (BS) threshold of 50, above which branches of a tree are considered reliable rather than artifacts of estimation error. After concatenation of the individual loci assigned to a bin into 883 'supergene alignments', we again performed best-tree and bootstrap searches on these supergenes (partitioned by UCE locus) using RAxML. For bins with only one assigned locus (N = 419), we instead retained previously estimated gene trees. We weighted the supergene trees by their size, i.e., a supergene of bin size x had a representation of x in the tree set used for analysis. Finally, we performed coalescent species-tree analysis in ASTRAL-II v4.10.10 (Mirarab and Warnow 2015) using the weighted 464 supergene trees and the 419 previously estimated gene trees.

Analyses of data subsets

We calculated average BS and tree length using R scripts from (Borowiec et al. 2015) (available at https://github.com/marek-borowiec/metazoan_phylogenomics/blob/master/gene_stats.R) and calculated similar alignment statistics with AMAS (Borowiec 2016) for each of the 1,763 individual gene trees as we did for the concatenated data set. We condensed the set of 1,763 gene trees to a subset of 50 loci with the highest average bootstrap score across all nodes in the gene tree ('50-best') for use in dating analyses. We also selected two sets of 50 loci randomly to test against potential bias in this 50-best data set. We used the *r cluster* algorithm and PartitionFinder2 (Frandsen et al. 2015, Lanfear et al. 2017) for the selection of the best partitioning scheme from these subsets, resulting in 37 partitions for the UCE-50-best, 38 partitions for the '50-random-1', and 40 partitions for the '50-random-2' subset.

Dating Analyses

We inferred divergence dates within Crematogastrini from the subset of '50-best' UCE loci (as described above), as well as from the two subsets of '50-random' loci using BEAST2 v2.3.2 (Bouckaert et al. 2014) run via the SI/HPC. Analyses incorporated data partitioning as estimated by the greedy algorithm in PartitionFinder2. We used two alternative starting trees: 1) the best tree resulting from the concatenated RAxML analysis with 1,763 partitions and 2) the species tree estimated by ASTRAL-II (used in combination with 50-best data set only). Due to computational constraints, topology was fixed during analyses to these starting trees by setting weight = 0 for all operators acting on the tree model. Four runs each for the 50-best data and two runs each for the 50-random data sets were employed with a chain length of 220–300 million generations. We imposed a diffuse gamma distribution on the mean branch lengths (ucld.mean; alpha = 0.001, beta = 1,000) and set the starting value for the clock rate = 1e-9, but otherwise left priors at their default values. We chose a Yule tree prior and defined lognormal calibration priors based on seven calibrations used by Ward et al. (2015) (see Supp Table 2 [online only]); however, we incorporated an updated younger estimate for Baltic amber (Aleksandrova and Zaporozhets 2008) and Sicilian amber (LaPolla et al. 2013) into these calibration priors. An important consideration when using lognormal calibration priors for divergence dating is how the user-specified calibration priors interact with the tree prior to form the marginal prior (or joint prior) on the calibrated node, and further how this marginal prior influences the posterior distribution in the light of the data (Brown and Smith 2017). We therefore also performed an analysis sampling only from the marginal prior (running an 'empty' analysis without data) in order to confirm that 1) the marginal prior distributions were similar to our user-specified calibration prior and 2) the data were informative enough to return posterior distributions different from the marginal priors. We did this by visually inspecting distributions in Tracer v1.6. We analyzed trace files in Tracer v1.6 to determine chain convergence and burn-in, and after discarding a burn-in of at least 20%, summarized 36,300–84,300 trees as maximum clade credibility (MCC) trees using LogCombiner v2.4.3 and TreeAnnotator v2.4.3.

Biogeographic Analyses

We inferred the biogeographic history of Crematogastrini using BioGeoBEARS (Matzke 2013). We focused hereby exclusively on the genus level to avoid any bias caused by species ranges being

either overrepresented or absent from our phylogeny. While this is a rather coarse approach to biogeographic reconstruction, we believe this is appropriately conservative given our taxon sampling. We thus coded geographic distributions for each genus based on the distribution of all of its described members (see Supp Table 3 [online only]). Given the disagreements between classification and phylogeny for some genera, we assigned *Ancyridris polyrhachioides* Wheeler, *Propodilobus pingorum* DuBois, and the three *Lasiomyrma* Terayama & Yamane species to a more inclusive *Lordomyrma* Emery s.l. clade. *Strongylognathus testaceus* Schenck was further included within *Tetramorium* Mayr. We designated seven biogeographic areas (Neotropical, Nearctic, Palearctic, Afrotropical, Malagasy, Indomalayan, and Australasian [after Cox 2001]), and defined dispersal constraints based on the level of connectivity between these landmasses using slightly different rates for two distinct time periods from 0–50 Ma and 50–80 Ma (see Supp Table 4 [online only]). We prepared a modified chronogram from each of the 50-best analyses based on the concatenated (50-best-CP) and the species-tree (50-best-ST) topologies by pruning all but one representative species per genus, as well as the outgroups from the tree. We used these phylogenies, the genus-level distribution matrix, and the constraint matrix as input for two sets of BioGeoBEARS analyses (50-best-CP and 50-best-ST) following guidelines and tutorials available on the BioGeoBEARS PhyloWiki (http://phylo.wikidot.com/biogeobears). For both sets of analyses, we implemented the standard two-parameter dispersal and extinction cladogenesis (DEC) model (Ree and Smith 2008), as well as the DEC+J version of the former model that incorporates founder-event speciation by assigning a separate probability parameter 'j' (Matzke 2014). We defined max_range_size = 7, since a few genera occupy all seven biogeographic areas. The starting value for the founder-event speciation parameter 'j' was specified with jstart = 0.0001. We compared the fit of these models with a log-likelihood ratio test and repeated each analysis twice, obtaining identical results each time.

Diversification Rate Estimation

We estimated whether shifts in diversification rates occurred over time in the evolution of Crematogastrini using BAMM v2.5 (Rabosky et al. 2013, Rabosky 2014) and the associated R package BAMMtools v2.1.5 (Rabosky et al. 2014). We accounted for incomplete sampling by using clade-specific sampling probabilities. For these we assembled a species-richness matrix listing 1) the diversity of described species and 2) the diversity of described species and subspecies for each genus (see Supp Table 5 [online only]). We then accordingly created two clade-specific sampling probability matrices by assigning each tip (i.e., a species) in our phylogeny to a clade and assigned this clade a sampling fraction calculated as the number of sampled species divided by number of described species (or species + subspecies) in that clade (see Supp Table 5 [online only]). Most species were assigned to a clade equivalent to their respective genus, except we again used a more inclusive definition for the *Lordomyrma* s.l. clade (see above) and *Tetramorium*. We used the two UCE-50-best chronograms based on the concatenated and coalescent species-tree topologies plus these two sets of sampling fractions to perform four different sets of BAMM analyses. We configured our analyses using the guidelines in the BAMM documentation (http://bamm-project.org/). We used the function 'setBAMMpriors' within BAMMtools to obtain appropriate priors for speciation-extinction analyses, and the expected number of shifts was left at the default value (=1). Our runs included four MCMC chains with a length of 50 million generations, sampling every 10,000 generations. We discarded a burn-in of 10% and confirmed that effective sample size values were appropriate (1,400–2,400). Results were analyzed and plotted with various functions in BAMMtools as follows. We used computeBayesFactors to identify the best-supported model of rate shifts in our data. We plotted the maximum a posteriori probability (MAP) shift configuration (getBestShiftConfiguration), the 95% credible set of distinct rate shift configurations (credibleShiftSet), and a 'phylorate' graph showing mean marginal posterior density of speciation rates (plot.bammdata).

Nesting Preference

To estimate the ancestral state of nesting preference in the Crematogastrini, we scored each genus by its members' combined nesting habits as either ground-dwelling, arboreal, or generalist (i.e., occupying both arboreal and ground habitats). Sixteen genera were thus scored as being exclusively arboreal, 35 as ground-dwelling, and five as generalists (Supp Table 3 [online only]), based on information we gathered from the literature, specimen records on AntWeb, and personal collecting experience. We used the rayDISC function in the R package corHMM (https://www.R-project.org/) to reconstruct ancestral states for these trait categories. We performed reconstructions under the 'equal rates' (ER) model and the 'all rates different' (ARD) model and compared the fit of these models by performing a likelihood ratio test on the resulting –lnL scores as *(1-pchisq(Δ lnL, df))*. All reconstructions were performed using both the 50-best-CP and the 50-best-ST chronogram.

Results

UCE Data Characteristics

Due to the large age range of our specimens, the concentrations of our DNA extractions ranged from <0.05 to 27.1 ng/µl (average 2.1 ng/µl). Our post-library preparation DNA concentrations were equally variable, ranging from 0.3 to 105 ng/µl (average 32.5 ng/µl). From the enriched libraries, we were able to generate 13,667–5,845,581 reads per taxon (average: 2,279,011), which Trinity assembled into 136–228,374 contigs (average: 59,518) of average length 235–606 bp per taxon (average across taxa: 347 bp) and 4–28.1× coverage (average: 9.4×). The assembled contigs matched 103–2399 UCE loci (average: 2200 loci after removal of duplicates in Phyluce) with an average length of 229–1049 bp per taxon (average across taxa: 654 bp) and 4.7–123.2× coverage (average: 42.1×). Between 0.13 and 0.94 reads (average: 0.42) were on target. The overall lowest results were obtained from a *Lordomyrma epinotalis* specimen that had already undergone a nondestructive DNA extraction procedure for a different study (Lucky and Sarnat 2010); it was re-extracted by us due to the lack of other available material. Details on the library concentrations and UCE capture values can be found in Supp Table 6 (online only). We calculated several descriptive statistics from our complete alignment (90% matrix, 1,763 loci), as well as for the data subsets used in the dating analysis, which are listed in Supp Table 7 (online only). In brief, our complete data matrix had a length of 913,718 bp with 18% missing data, 59% variable sites, and 49% parsimony-informative characters. The GC heterogeneity score across taxa in the alignment is relatively low at 1.2%, and mean GC content is moderate at 44%.

Phylogeny of Crematogastrini

We inferred phylogenetic relationships within the tribe Crematogastrini using a concatenated ML approach (both partitioned by locus and unpartitioned), as well as by reconstructing a species tree estimated from 1,763 UCE gene trees (binned into 883 'supergenes'). Both methods returned tree topologies that were overall well supported and

largely congruent (Figs. 1 and 2), with the few exceptions described below. In all analyses, *Rostromyrmex pasohensis* Rosciszewski is estimated as the sister lineage to all remaining Crematogastrini. Based on the concatenated ML tree, we further identify 10 main clades within Crematogastrini that have good or full support (BS: 79–100), here treated as informal genus-groups. Eight of these groups are recovered, with maximum support, in the species-tree topology but two of them become paraphyletic in that analysis (Fig. 2).

1) *Formicoxenus* genus-group: *Vombisidris* Bolton, *Gauromyrmex* Menozzi, *Harpagoxenus* Forel, *Leptothorax* Mayr, *Formicoxenus* Mayr, and *Temnothorax* Mayr.

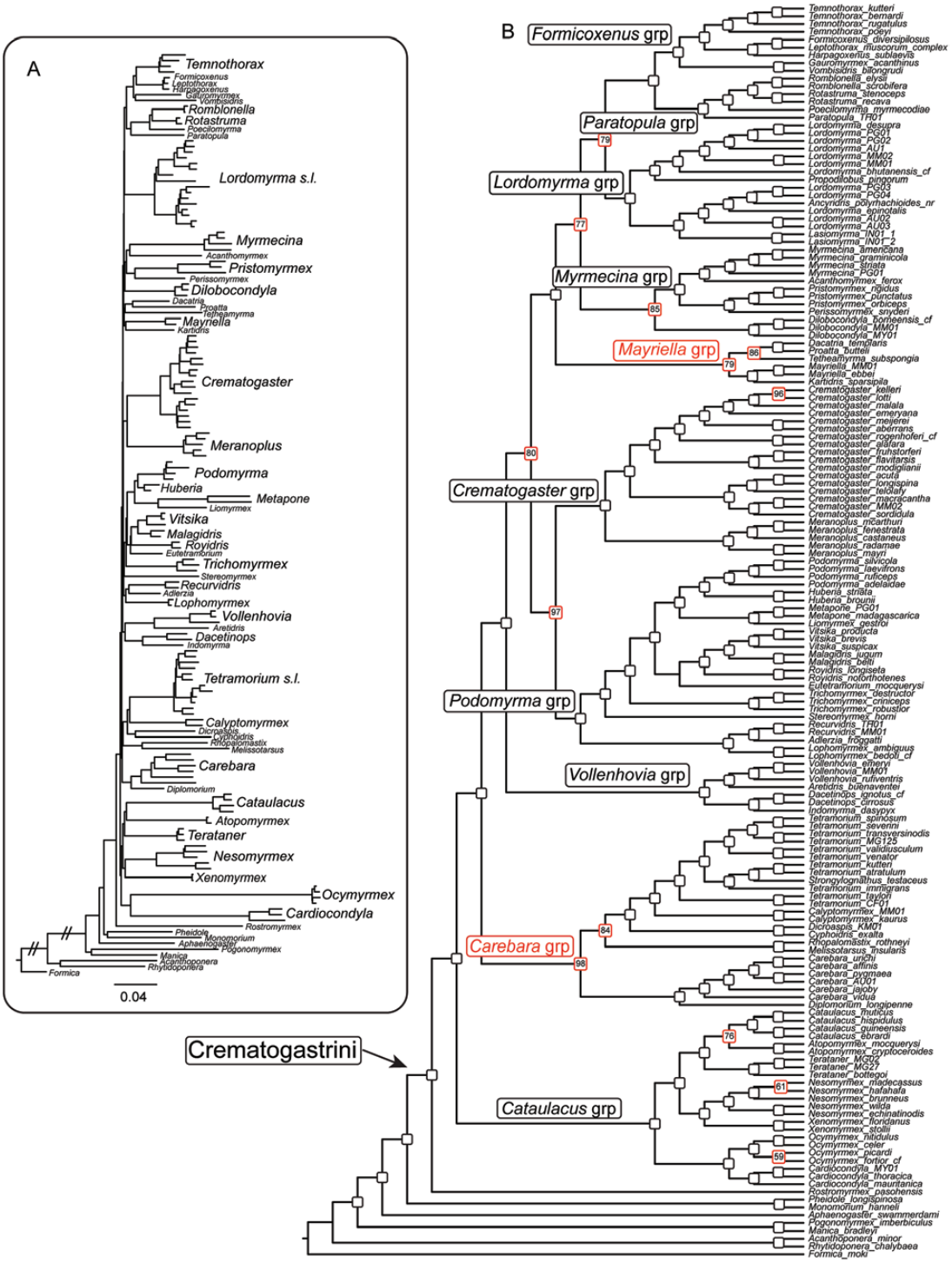

Fig. 1. Phylogeny of Crematogastrini, estimated by concatenated ML analysis. We performed best-tree and bootstrap searches ($N = 100$) in RAxML v8.2.7. Both panels show the best ML tree resulting from analyses of a concatenated data matrix divided per UCE locus into 1,763 partitions. (A) Phylogram showing branch lengths and emphasizing generic relationships. (B) Cladogram with BS values indicated: white squares represent 100% BS; red squares indicate the support for that node. The 10 major genus-groups are indicated; the compositions of the two genus-groups highlighted in red conflict with those resulting from the ASTRAL-II analysis presented in Fig. 2.

Fig. 2. Cladogram estimated for Crematogastrini, by ASTRAL-II species-tree analysis. We reconstructed a species tree from 1,763 UCE gene trees based on weighted statistical binning (Bayzid et al. 2015) and 883 supergenes. Only local posterior probabilities (LPP) > 0.7 are shown. Note that ASTRAL-II support values are branch support values that measure the support for a quadripartition, not a bipartition. The 10 major genus-groups are indicated; clade names in red highlight conflicts regarding the composition of these clades with respect to Fig. 1.

2) *Paratopula* genus-group: *Paratopula* Wheeler, *Poecilomyrma* Mann, *Rotastruma* Bolton and *Romblonella* Wheeler.
3) *Lordomyrma* genus-group: *Lordomyrma* sensu lato, including *Lordomyrma*, *Lasiomyrma*, *Propodilobus* Branstetter, and *Ancyridris* Wheeler. It is obvious from our analyses that *Lordomyrma* as presently defined is paraphyletic with respect to the other three genera. The results from species-tree analyses place *Lordomyrma* sensu lato within a paraphyletic *Mayriella* genus-group (Fig. 2).
4) *Myrmecina* genus-group: *Myrmecina* Curtis, *Acanthomyrmex* Emery, *Pristomyrmex* Mayr, *Perissomyrmex* Smith, and *Dilobocondyla* Santschi.
5) *Mayriella* genus-group: *Kartidris* Bolton, *Mayriella* Forel, *Tetheamyrma* Bolton, *Proatta* Forel, and *Dacatria* Rigato.
6) *Crematogaster* genus-group: *Crematogaster* Lund and *Meranoplus* Smith.
7) *Podomyrma* genus-group: *Lophomyrmex* Emery, *Adlerzia* Forel, *Recurvidris* Bolton, *Stereomyrmex* Emery, *Trichomyrmex* Mayr, *Eutetramorium* Emery, *Royidris* Bolton & Fisher, *Malagidris* Bolton & Fisher, *Vitsika* Bolton & Fisher, *Liomyrmex* Mayr, *Metapone* Forel, *Huberia* Forel, and *Podomyrma* Smith.
8) *Vollenhovia* genus-group: *Vollenhovia* Mayr, *Indomyrma* Brown, *Dacetinops* Brown & Wilson, and *Aretidris* General.
9) *Carebara* genus-group: *Diplomorium* Mayr, *Carebara* Westwood, *Dicroaspis* Emery, *Cyphoidris* Weber, *Tetramorium*, *Rhopalomastix* Forel, and *Melissotarsus* Emery. In the species-tree topology, *Rhopalomastix* and *Melissotarsus* form a separate but adjacent lineage, rendering this genus-group paraphyletic (Fig. 2).
10) *Cataulacus* genus-group: *Cardiocondyla*, *Ocymyrmex*, *Nesomyrmex* Wheeler, *Terataner*Forel, *Atopomyrmex* André, *Xenomyrmex* Forel, and *Cataulacus* Smith.

Aside from the alternative topologies for the *Carebara* genus-group and the *Mayriella* genus-group, concatenated and species-tree approaches show only one other major disagreement: in the concatenated topology, the *Crematogaster* genus-group is sister to the *Podomyrma* genus-group with fairly high support (BS: 97; Fig. 1B), whereas the species-tree analysis estimates a ladderized topology and does not support a sister-group relationship between these two clades (Fig. 2). We also performed an unpartitioned analysis on the concatenated data set to test whether our partitioning strategy had an influence on the results. This unpartitioned ML analysis returned a tree very similar to the above partitioned analyses, with the notable exception that *Cardiocondyla* and *Oxymyrmex* jump outside the *Carebara* genus-group as a separate lineage, sister to the remaining Crematogastrini (but exclusive of *Rostromyrmex*) (Supp Fig. 1 [online only]).

Since *Rostromyrmex*, *Cardiocondyla*, and *Ocymyrmex* are subtended by relatively long branches, we explored the possibility that LBA affects the placement of these taxa, as well as the influence of these taxa on tree topology in general, by sequentially excluding them from the analysis. The results of these exclusion tests are depicted in schematic format in Supp Fig. 2 (online only). Excluding *Rostromyrmex* from the analysis had no effect on topology or support with regard to the remaining ingroup taxa (Supp Fig. 2A [online only]), nor did the exclusion of *Cardiocondyla* (Supp Fig. 2C [online only]) or *Ocymyrmex* and *Cardiocondyla* at the same time (Supp Fig. 2D [online only]). In contrast, excluding *Ocymyrmex* from the analysis eroded support for the *Cataulacus* genus-group clade, resulting in a position of *Cardiocondyla* outside of this clade, grouping as sister to the remaining Crematogastrini (exclusive of *Rostromyrmex*). This alternative topology, however, received little support (bootstrap proportion: 44; Supp Fig. 2B [online only]).

Timing of the Evolution of Crematogastrini

Using BEAST2 and a reduced data set of 50 UCE loci, we estimated the timescale of the evolution of Crematogastrini. We estimated ages from 50 loci with the best average bootstrap score (50-best) for both the concatenated and species-tree topologies (concatenated-partitioned: 50-best-CP; species tree: 50-best-ST). We also compared these age estimates to divergence ages estimated from two sets of randomly chosen loci (50-random-1, 50-random-2) to assure that the 50-best data set did not result in biased divergence ages. Table 1 compares divergence estimates from these four analyses for the main clades within Crematogastrini, as well as for all genera for which crown-group estimates were obtained. Complete chronograms with age estimates and 95% highest posterior density intervals can be found in the supplementary material (Supp Figs. 3–6 [online only]). Overall, we received highly congruent age estimates from the four analyses, differing between <1 and 5.7 Ma (Table 1). The only exception is the crown-group age of *Dacetinops*, which was estimated ca. 20 Ma younger from the 50-random-1 and 50-random-2 data sets than from the 50-best-CP and 50-best-ST data sets. Differences between the concatenated and species-tree topologies did not appear to affect age estimates significantly. For example, the *Lordomyrma* genus-group, while estimated in a different position in the two analyses, is estimated with a crown age of 38.3 and 37 Ma in the 50-best-CP and 50-best-ST analysis, respectively.

Crown-group Crematogastrini are estimated in our analyses to have evolved ~75.3–79.4 Ma in the late Cretaceous. This is remarkably close to the estimate of 70.8 Ma obtained in the larger analysis of the subfamily Myrmicinae by Ward et al. (2015)—especially considering that study did not include *Rostromyrmex*, the earliest-branching taxon in our analysis. Diversification into the 10 main clades that we recognize here took place mainly in the late Cretaceous to early Eocene between 50 and 70 Ma, with the exception of the *Lordomyrma* genus-group, which is somewhat younger with an estimated age of 37–40 Ma. The Oligocene and Miocene were important settings in generating the presently recognized generic diversity of Crematogastrini, as the majority of genera appear to have evolved between 8 and 31 Ma. Notably older, with Eocene crown-age estimates, are *Carebara* (46.8 Ma), *Nesomyrmex* (40.5 Ma), and *Crematogaster* (39.3 Ma). A few genera are estimated as being of very young crown-group age, such as *Ocymyrmex* (5.8 Ma), *Atopomyrmex* (3.1 Ma), *Lophomyrmex* (4 Ma), *Rotastruma* (4.4 Ma), and *Romblonella* (1.8 Ma). These estimates must be viewed with caution as they could be influenced by incomplete taxon sampling.

Biogeography

We used BioGeoBEARS (Matzke 2013) to infer the early biogeographic history of Crematogastrini from the 50-best-CP and 50-best-ST chronograms. We compared the fit of the standard two-parameter DEC model (Ree and Smith 2008) with the DEC+J model incorporating founder-event speciation. The DEC+J model did not provide a significantly better fit in either of the two alternative analyses; therefore, we focus on discussing results estimated from the standard DEC model. Biogeographic reconstructions are highly congruent between the two alternative topologies (Fig. 3A; Supp Fig. 7A [online only]). The ancestral range of Crematogastrini is estimated in the Afrotropical and Indomalayan regions, which also remain the two dominant ancestral distributions during much of the early evolution of the tribe. However, in the very early evolution of Crematogastrini the affinity with the Indomalayan region is indicated only by the phylogenetic position of the enigmatic Malaysian endemic and monotypic genus *Rostromyrmex*. The *Cataulacus* genus-group and the *Carebara* genus-group are inferred to have evolved mainly in the Afrotropical region, with a possible dispersal to the Neotropics by the ancestor of *Nesomyrmex* and *Xenomyrmex* between 62 and 68 Ma, and a dispersal to the Indomalayan region by *Rhopalomastix* sometime in the Eocene (after 45 Ma). This scenario would imply dispersal back to the Afrotropics by one *Nesomyrmex* lineage. All remaining eight clades are estimated to share a common ancestor restricted to the Indomalayan region. Further lineage diversification appears to have taken place exclusively in this region until ca. 65 Ma or later, when an ancestor of *Adlerzia*, *Recurvidris*, and *Lophomyrmex* dispersed to Australasia. Other notable dispersal events in the early history of Crematogastrini are inferred within the *Podomyrma* genus-group. Here, one dispersal of an ancestor of the four Malagasy endemic genera *Eutetramorium*, *Royidris*, *Malagidris*, and *Vitsika* to the Malagasy region is supported between 50 and 60 Ma, as is another dispersal event around the same time in the sister lineage comprised of *Liomyrmex*, *Metapone*, *Huberia*, and *Podomyrma*. For the latter, while the ancestral reconstructions remain ambiguous, an initial dispersal from the Indomalayan to the Australian region is probably most likely: *Podomyrma* and *Huberia* are Australasian taxa (*Huberia* is a New Zealand endemic; *Podomyrma* occurs in Australia and New Guinea), *Liomyrmex* occurs in southeast Asia and New Guinea, and only *Metapone* extends to the African and Malagasy regions. Again prior to ca. 50 Ma, a dispersal to the Paleotropical region is estimated within the *Formicoxenus* genus-group, followed by a subsequent dispersal to the Nearctic. The early evolution of the remaining clades (*Vollenhovia* genus-group, *Crematogaster* genus-group, *Mayriella* genus-group, *Lordomyrma* genus-group, *Myrmecina* genus-group, and *Paratopula* genus-group) was found to be heavily centered in the

Table 1. Divergence age estimates for major clades (bolded) and genera within Crematogastrini

	Concatenated-partitioned (CP)			Species tree (ST)	
Node	50-best	50-random-1	50-random-2	50-best	Average
Crematogastrini	**78.6**	**75.4**	**79.4**	**78.7**	**78.0**
***Formicoxenus* genus-group**	**52.4**	**49.8**	**51.2**	**52.8**	**51.5**
Temnothorax	19.1	18.2	19.3	19.6	19.0
***Paratopula* genus-group**	**52.3**	**52.3**	**52.3**	**52.6**	**52.4**
Rotastruma	3.6	4.9	5.5	3.6	4.4
Romblonella	1.4	1.5	2.7	1.4	1.8
***Lordomyrma* genus-group**	**38.3**	**38.9**	**39.5**	**37.0**	**38.4**
***Myrmecina* genus-group**	**62.9**	**62.3**	**63.1**	**62.5**	**62.7**
Dilobocondyla	13.5	15.5	15.8	13.6	14.6
Perissomyrmex, Pristomyrmex	51.6	51.4	52.0	51.6	51.6
Pristomyrmex	30.5	30.6	30.6	31.6	30.9
Acanthomyrmex, Myrmecina	52.7	53.9	55.9	52.5	53.7
Myrmecina	22.3	25.7	25.2	22.2	23.8
***Mayriella* genus-group**	**64.0**	**63.8**	**64.0**	**Not supported**	**63.9**
Kartidris, Mayriella	60.5	59.8	62.3	60.3	60.7
Mayriella	14.9	12.7	12.9	14.4	13.7
Proatta, Dacatria	51.1	50.2	49.2	51.2	50.4
***Mayriella* genus-group and *Lordomyrma* s.l.**		**Not supported**		**64.8**	**64.8**
***Crematogaster* genus-group**	**59.7**	**60.6**	**61.8**	**60.0**	**60.5**
Meranoplus	22.5	21.3	24.6	23.5	23.0
Crematogaster	38.5	39.0	41.0	38.8	39.3
***Podomyrma* genus-group**	**65.8**	**63.1**	**64.8**	**66.2**	**65.0**
Lophomyrmex	4.4	4.0	3.4	4.4	4.0
Adlerzia, Recurvidris	57.5	52.5	54.6	57.7	55.6
Recurvidris	14.1	15.6	15.0	14.2	14.7
Trichomyrmex	21.9	20.0	20.5	22.7	21.3
Royidris	8.4	7.5	10.7	8.5	8.8
Malagidris	14.5	11.9	17.6	14.6	14.6
Vitsika	21.5	18.3	21.8	22.6	21.0
Liomyrmex, Metapone	36.9	37.7	38.0	38.0	37.6
Metapone	20.0	21.1	21.1	21.2	20.9
Huberia	16.9	15.0	13.5	16.7	15.5
Podomyrma	12.0	13.6	13.6	12.1	12.8
***Vollenhovia* genus-group**	**62.5**	**62.0**	**63.9**	**62.3**	**62.7**
Indomyrma, Dacetinops	44.4	41.1	43.0	44.4	43.2
Dacetinops	27.9	8.6	9.5	28.1	18.5
Aretidris, Vollenhovia	44.8	44.1	45.5	43.7	44.5
Vollenhovia	25.1	22.7	23.3	23.9	23.7
***Carebara* genus-group**	**68.0**	**65.8**	**69.6**	**Not supported**	**67.8**
Diplomorium, Carebara	55.7	56.4	58.3	55.5	56.5
Carebara	46.0	46.5	48.7	46.0	46.8
Rhopalomastix, Melissotarsus	45.0	45.6	48.8	46.5	46.5
Dicroaspis, Cyphoidris	49.7	44.1	49.2	49.3	48.1
Calyptomyrmex	16.4	14.5	16.2	15.8	15.7
Tetramorium	25.3	23.1	26.1	25.3	24.9
Carebara* genus-group excl. *Rhopalomastix, Melissotarsus		**Not supported**		**67.7**	**67.7**
***Cataulacus* genus-group**	**70.5**	**68.6**	**69.6**	**70.7**	**69.8**
Cardiocondyla	28.9	26.4	27.6	28.6	27.9
Ocymyrmex	4.8	7.4	6.6	4.7	5.8
Nesomyrmex	40.6	39.8	41.2	40.6	40.5
Terataner	6.1	10.2	10.8	6.2	8.3
Atopomyrmex	2.3	5.3	2.5	2.3	3.1
Cataulacus	20.4	19.0	18.3	20.1	19.5

We estimated ages from different data sets and topologies: using the 50-best, 50-random-1, and 50-random-2 data sets while employing a tree topology estimated from a concatenated-partitioned analysis of the entire 1,763-locus data set, and using the 50-best data set while employing the species-tree topology. Ages given are median heights. Genera for which no crown-group ages could be estimated are omitted.

Indomalayan region. Further dispersal events explaining the broader present-day distributions of some crematogastrine genera are therefore likely associated with species-level diversification events not captured by our biogeographic study.

Evolution of Nesting Preference

The ER model was estimated to provide the best fit to our nesting preference data, and tree topology had only a minor effect on state reconstructions. We found overwhelming support for a ground-dwelling

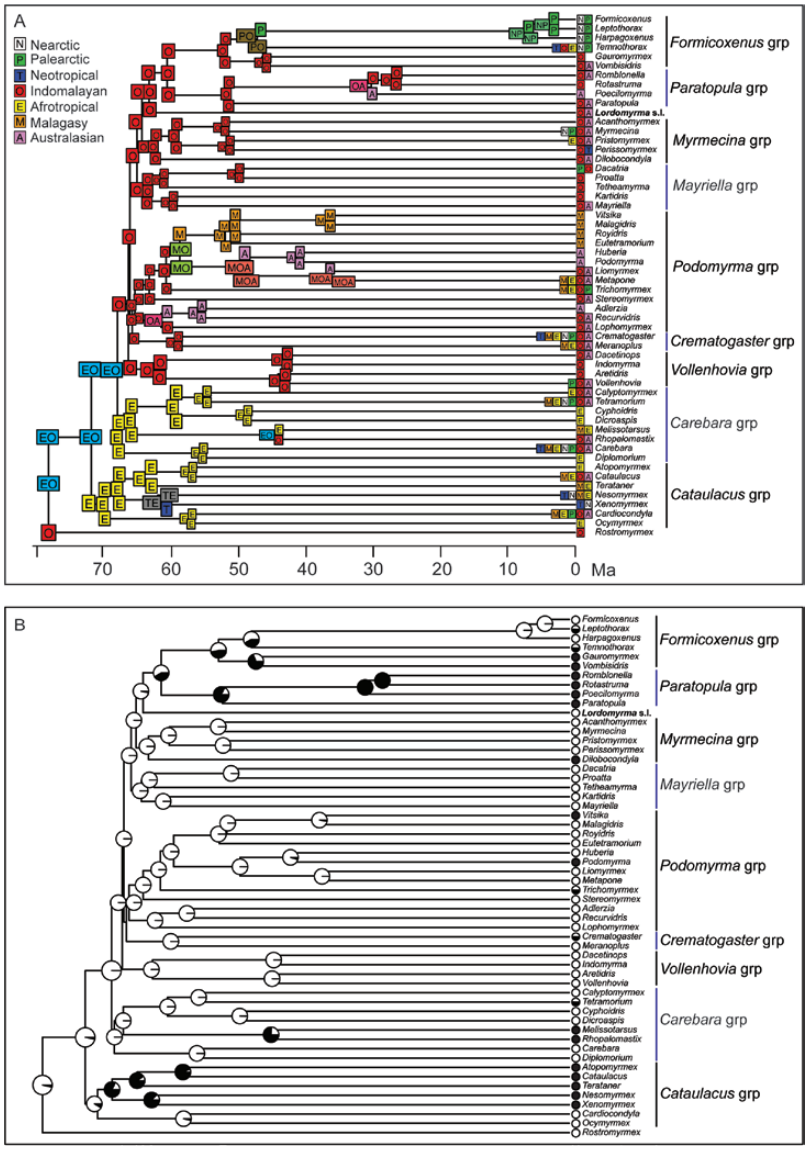

Fig. 3. The evolution of biogeography (A) and nesting preference (B) in Crematogastrini. Ancestral reconstructions based on a modified chronogram from the 50-best concatenated-partitioned analysis in BEAST2, from which all but one representative species per genus, as well as the outgroups, have been pruned from the tree. (A) Biogeographic reconstructions with BioGeoBEARS under the DEC model. N = Nearctic, T = Neotropical, P = Palearctic, E = Afrotropical, M = Malagasy, O = Indomalayan, and A = Australasian. (B) Nesting preference reconstructed under the ER model with rayDISC in corHMM. Black = arboreal nesting; white = ground nesting. See Supp Table 3 (online only) for geographic distributions and trait data for each genus.

ancestor of Crematogastrini, which is probably unsurprising given that the majority of the genera within the tribe are ground-dwelling. A more interesting result is the good support for four lineages of exclusively arboreal genera: 1) the subclade within the *Cataulacus* genus-group including *Xenomyrmex*, *Nesomyrmex*, *Cataulacus*, *Teratataner*, and *Atopomyrmex*; 2) *Rhopalomastix* and *Melissotarsus* (part of the *Carebara* genus-group); 3) the *Paratopula* genus-group; and 4) *Vombisidris* and *Gauromyrmex* (part of the *Formicoxenus* genus-group). There is further weak support (PP = 0.4–0.5, Fig. 3B; Supp Fig. 7B [online only]) for an arboreal nesting preference in the most recent common ancestor (MRCA) of the *Formicoxenus* and *Paratopula* genus-groups. Otherwise, exclusive arboreality has evolved independently only in three other genera, *Dilobocondyla*, *Podomyrma*, and *Vitsika*. Four or five genera have adapted to a generalist lifestyle from a ground-dwelling ancestor: *Crematogaster*, *Tetramorium*, *Trichomyrmex*, *Leptothorax*, and *Temnothorax*, with the ancestral state of the latter being somewhat ambiguous.

Genus-Level Diversification of Crematogastrini

We estimated rates of diversification in Crematogastrini and investigated whether significant rate shifts have occurred over time, using the 50-best-CP and 50-best-ST topologies and two sets of sampling fractions based on species estimates that either excluded or included subspecies. We plotted the mean marginal posterior density of speciation rates for the four different analyses in Fig. 4A and B and Supp Fig. 8A and B (online only). These phylorate graphs show an increase in estimated rate in all analyses along the branches leading to five genera: *Crematogaster*, *Meranoplus*, *Tetramorium*, *Temnothorax*, and *Ocymyrmex*. The highest rate increase occurs along the branch leading to *Tetramorium*. The two analyses including subspecies further estimate a higher rate increase along the branch leading to *Crematogaster* than analyses excluding subspecies. The best-supported rate shift configuration estimated three shifts occurring throughout the diversification of Crematogastrini, regardless of

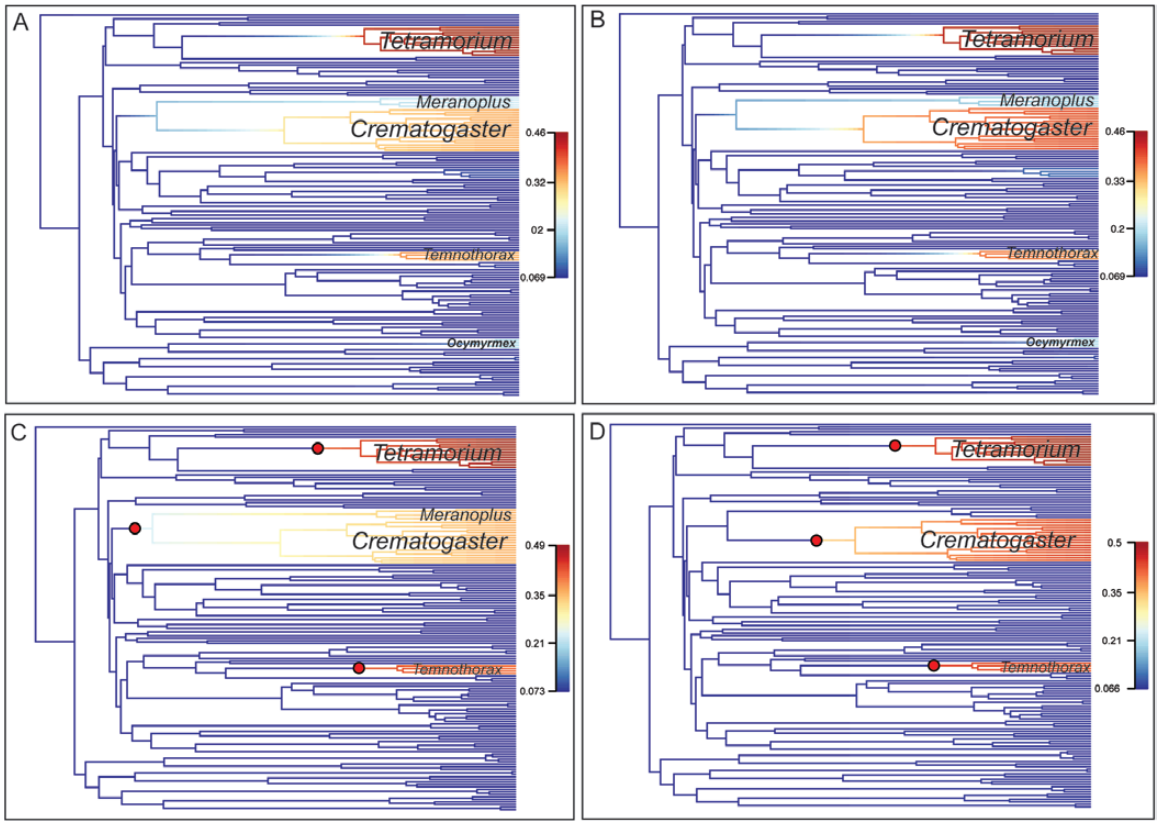

Fig. 4. Diversification of Crematogastrini. We performed BAMM analyses on the chronogram resulting from the 50-best concatenated-partitioned BEAST2 analysis using clade-specific sampling probabilities to account for incomplete sampling based either on species estimates only or including species and subspecies. Panels show (A) mean phylorate plots based on species only; (B) mean phylorate plots based on species and subspecies; (C) best shift configuration based on species only; (D) best shift configuration based on species and subspecies. Supp Table 5 (online only) lists diversity estimates per genus including and excluding subspecies.

which topology and species estimate was used (Fig. 4C and D; Supp Fig. 8C and D [online only]). The four analyses all agree on the position of two of these rate shifts: one is placed on the branch leading to *Tetramorium* and one on the branch leading to *Temnothorax*. The third shift is placed on either the branch leading to *Crematogaster* (50-best-CP analysis including subspecies, 50-best-ST analyses excluding/including subspecies; Fig. 4D; Supp Fig. 8C and D [online only]) or the branch leading to the *Crematogaster–Meranoplus* clade (50-best-CP analysis excluding subspecies, Fig. 4C). However, the frequency (=posterior probability support) for the best shift configuration was low in all four cases (f = 0.2–0.27), and several other slightly different credible shift configurations were found (Supp Figs. 9–12 [online only]).

Discussion

The ant tribe Crematogastrini is a highly diverse group, accounting for approximately 20% of all described species of ants. A previous Sanger-sequencing study (Ward et al. 2015) was unable to clarify relationships in deeper parts of the tree. Our use of targeted genome enrichment, augmented by improved taxon sampling, results in a much better resolved phylogeny (Figs. 1 and 2) and allows us to identify 10 major clades within the tribe that have moderate to strong support. These can serve as useful reference points in future investigations. The new phylogeny does not contradict any well-supported clades in the earlier study (Ward et al. 2015) but does uncover many novel relationships including 1) the placement of *Rostromyrmex* as sister to all other Crematogastrini, 2) a sister-group relationship between the *Formicoxenus* genus-group and the *Paratopula* genus-group, 3) monophyly of the *Myrmecina* genus-group, with *Dilobocondyla* sister to the other four genera, 4) monophyly of a large clade—here called the *Podomyrma* genus-group—that contains more than a dozen African and Indo-Australian genera, 5) recovery of another large clade, the *Carebara* genus-group, that includes such diverse genera as *Tetramorium*, *Calyptomyrmex*, and *Carebara*, and 6) consistent relationships among the 10 major clades. The present study also affirms the existence of clades that previously had only weak or ambiguous support such as a *Cardiocondyla* + *Ocymyrmex* and *Crematogaster* + *Meranoplus*.

Biogeography

Divergence dating and biogeographic inferences suggest a Paleotropical origin for the Crematogastrini at approximately 75 Ma. The 10 major lineages recognized here arose over a relatively limited time interval (50–70 Ma) in the Afrotropical and Indomalayan regions. This was a period of warm, equable climate (Zachos et al. 2008, Archibald et al. 2013) when many of the major angiosperm clades also originated, especially among eudicots (Tank et al. 2015). Most extant genera of Crematogastrini have estimated crown ages of 10–40 Ma, i.e., they appear to have originated after the early Eocene climatic optimum (Zachos et al. 2001) under generally cooler and drier conditions, and again predominantly in the Old World. A few genera, such as *Carebara*, *Crematogaster* (Blaimer 2012), and *Temnothorax* (Prebus 2017), have infiltrated the New

World, but it is striking how the main theater of crematogastrine evolution has been the Paleotropics, especially the Indomalayan region. Of the 10 genus-group lineages we recognize in this study, the majority (eight) are inferred to have an Indomalayan origin, and only two, the *Cataulacus* and *Carebara* genus-groups, are reconstructed having an ancestral African distribution. Interestingly, the latter two are the earliest-branching lineages. However, given the enigmatic position of the Indomalayan genus *Rostromyrmex* as sister to the remaining Crematogastrini, the biogeographic origin of the tribe remains somewhat uncertain.

Within the *Podomyrma* genus-group, several dispersal events are inferred away from the Indomalayan region. First, a clade of four Malagasy endemic genera is inferred to have dispersed to that island before 50 Ma. This is an interesting result, since the only other time-calibrated study investigating dispersal of ants to Madagascar had suggested a much more recent origin for the genus *Crematogaster* (several dispersals to Madagascar after ~25 Ma; Blaimer 2012). Could the ancestor of these endemic groups have been the first ant to arrive in Madagascar? Neither of these four genera are currently very diverse (3–16 species). One might expect to see a burst of diversification coinciding with increased ecological opportunity if most ecological niches for ants had been freely available at the time of arrival. However, competition by more recently arriving lineages followed by extinction could have erased traces of an initial radiation of this Malagasy endemic ant clade. Some other reconstructions in the *Podomyrma* genus-group appear less biologically plausible given the present distribution of taxa and are probably a result of the genus-level coding used for distributions. For example, the MRCA of the clade consisting of *Podomyrma*, *Huberia*, *Liomyrmex*, and *Metapone* most likely had an Indomalayan and Australasian distribution (not Malagasy and Indomalayan), given the present-day distribution of these genera, and a dispersal to the Malagasy and Afrotropical region probably only happened much later within *Metapone* than our reconstructions suggest. Likewise, the inferred dispersal event of the MRCA of *Adlerzia*, *Recurvidris*, and *Lophomyrmex* to the Australasian region could be an artifact of assigning the Indomalayan and Australasian region equal weight in the distribution of *Recurvidris* and *Lophomyrmex* (by coding 'OA'). These genera are predominantly Indomalayan in distribution and only a few species cross Wallace's line into Australasia. Instead it is conceivable that only one dispersal event occurred along the stem lineage of *Adlerzia*, followed by separate recent dispersals within the other two genera.

Nesting Habitat Evolution

Ants successfully occupy a breadth of habitats and their vertical layers (canopy, leaf litter, and soil), yet these vary tremendously in microclimate and properties of nest sites. A significant distinction can usually be made between a community of arboreally nesting species and a community of ground-nesting species (living in the soil and leaf litter). A few larger ant genera have adapted to utilize both these vertical habitat layers (such as *Crematogaster*, *Tetramorium*, *Temnothorax*, and *Leptothorax* among Crematogastrini) but by and large we see fidelity in the choice for either one or the other. The question of whether the MRCA of all ants was arboreal or ground-dwelling, or in which habitat crown-group ants have evolved, has thus always piqued the curiosity of myrmecologists. Earlier hypotheses suggested the leaf litter was the cradle of ant evolution (Wilson and Hölldobler 2005, Perrichot et al. 2007). A subterranean, soil-dwelling ancestor was supported by the first formal analysis of this question, and the subfamily Myrmicinae was further reconstructed as ancestrally surface-dwelling (i.e., leaf litter) (Lucky et al. 2013). Perhaps unsurprisingly given these earlier results, we infer ground-dwelling (i.e., leaf litter and soil-dwelling) to be the ancestral condition in Crematogastrini. However, we discovered two larger clades within Crematogastrini that apparently have switched in whole to arboreal nesting: a clade within the *Cataulacus* genus-group comprising *Atopomyrmex*, *Cataulacus*, *Teratanes*, *Nesomyrmex*, and *Xenomyrmex*, as well as the entire *Paratopula* genus-group. For the latter, it is even possible (based on our reconstructions) that the switch occurred in the ancestor of the *Paratopula* and *Formicoxenus* genus-groups. Another switch to arboreal nesting occurred in the lineage comprising the enigmatic genera *Melissotarsus* and *Rhopalomastix*, which possess specialized silk-producing glands (although for *Rhopalomastix* the extent of silk production and use is not yet entirely confirmed; Hölldobler et al. 2014). We see a few switches to arboreality in other phylogenetically isolated genera (*Podomyrma*, *Vitsika*, and *Dilobocondyla*), but clearly overall arboreality has evolved in a nonrandom fashion in Crematogastrini. No switches from an exclusively arboreal nesting habit back to ground-nesting are supported (although some uncertainty remains within the *Formicoxenus*-group). This may indicate benefits of an adaptation to this habitat layer that prevent the retention of a generalist or reversal to a ground-dwelling lifestyle. More detailed species-level analyses estimating ancestral nest-site evolution within the 'generalist genera' (*Crematogaster*, *Tetramorium*, *Temnothorax*, and *Leptothorax*) are necessary, which in turn could lead to slightly different conclusions at the genus level.

Diversification of Crematogastrini

The subfamily Myrmicinae is the most species-rich and diverse lineage of ants in the world. A majority of this diversity is represented by the tribe Crematogastrini (together with the Attini), which contains three of the largest, most species-rich genera within the Myrmicinae: *Tetramorium*, *Crematogaster*, and *Temnothorax*. Three diversification rate shifts were inferred by our study and these shifts are associated unsurprisingly with these same three genera, which are also among the geographically most widespread taxa within Crematogastrini. A moderate diversification rate increase is further estimated for *Meranoplus* and *Ocymyrmex*, but with no distinct shifts supported. These two genera are fairly small, with 90 described species for *Meranoplus* and 34 species for *Ocymyrmex*. One explanation is that *Ocymyrmex* is estimated with a very young age (5.8 Ma), an estimate that could have been influenced by incomplete taxon sampling in our dating analyses (see above). We suspect that the evolutionary rate for this lineage is overestimated by our BAMM analyses. *Meranoplus* is the sister lineage to *Crematogaster*, and in one of the analyses (50-best-CP analysis excluding subspecies; Fig. 4C), a rate shift is placed on the branch subtending both *Meranoplus* and *Crematogaster*. Possibly *Meranoplus* shares some (but not all) of the characteristics with *Crematogaster* that led to increased diversification in this clade. Interestingly, in a larger-scale analysis estimating diversification rate across the ants (Blanchard and Moreau 2016), a positive shift in diversification rate is also placed on the branch leading to the *Crematogaster* and *Meranoplus* clade (rather than just *Crematogaster*). Further rate shifts in this study are placed in very similar locations on the Crematogastrini subtree; for example, as in our analysis, a positive shift in diversification rate for *Tetramorium* is recovered (Blanchard and Moreau 2016). However, the positive shift placed in our estimations on the *Temnothorax* branch is located in that study on the branch leading to a more inclusive clade of *Temnothorax*, *Leptothorax*, *Formicoxenus*, and *Harpagoxenus*, and is further estimated to be *negative*, resulting in a decreased diversification rate for the clade.

That study also recovers another negative shift leading to a clade comprised of *Proatta*, *Dacatria*, and *Tetheamyrma* (Blanchard and Moreau 2016). Presumably these differences in results compared to our study are influenced by taxon sampling, divergence dating, and the different methods used to estimate diversification rates (Medusa was used in Blanchard and Moreau 2016). The accuracy of BAMM in estimating diversification rates and rate shifts under certain circumstances has been recently debated. Moore et al. (2016) raised concerns about the sensitivity of BAMM analyses to the selected rate shift prior, which were convincingly countered by Rabosky et al. (2017). Additional criticism has been raised regarding a tendency to overestimate diversification rates in smaller clades, thereby resulting in a potential underestimation of rate shifts overall (Meyer and Wiens 2018). We conclude that our results are most likely not affected by potential erroneous diversification rate estimates, given that we recovered statistically significant shifts for the three most species-rich genera within Crematogastrini only—a result that essentially confirms observations based on taxonomic species diversity.

Positive shifts in diversification rate have usually been associated with either increased ecological opportunity, e.g., dispersal to and colonization of a new environment, or with the evolution of a key innovation, such as a novel trait (be it morphological, physiological, or genetic) that confers a competitive advantage to an organism or allows it to expand into a previously inaccessible environmental niche space. For example, turtle ants, genus *Cephalotes*, show an increase in diversification rate after colonizing a new habitat in the Chacoan region of South America (Price et al. 2014, Price et al. 2016). This positive rate shift was associated with phenotypic diversification in turtle ants (Price et al. 2016). Likewise, diving beetles (genus *Exolina*) were found to show a diversification rate shift after dispersing to Melanesia from Australia (Toussaint et al. 2015). Our results did not enable us to discern an association of the diversification rate shifts leading to *Crematogaster* and *Tetramorium* with a biogeographic dispersal event or an evolutionarily significant geological time period. However, potential biogeographic dispersal events *within* these genera may be responsible for these patterns, which would be masked by our generic-level approach to estimating diversification rates. With respect to the rate shift estimated for *Temnothorax*, if this shift would be more correctly located on the branch leading to the larger clade that includes *Leptothorax*, *Formicoxenus*, and *Harpagoxenus* (as estimated in Blanchard and Moreau 2016), a possible association with a dispersal of this clade from the Indomalayan to the Palearctic and Nearctic regions and a burst of diversification in these temperate regions is conceivable. Beyond a biogeographic dispersal, the colonization of additional nesting space could have led to increased diversification in these three groups. *Crematogaster*, *Temnothorax*, and *Tetramorium* have all evolved to nest both in ground and in arboreal habitats from an ancestrally ground-nesting state, and it seems plausible that the exploitation of the arboreal habitat has led to increased species diversification. For *Crematogaster*, morphological innovations also have been proposed to have led to the success of this genus. Synapomorphies for the genus are the dorsal attachment of the postpetiole to the fourth abdominal segment (first segment of gaster) and the absence of a dorsal petiolar node. These features give the ants the ability to flex the gaster forwards over the mesosoma while the petiole can be pressed tightly against the propodeum for protection (Buren 1959). *Crematogaster* workers also use this posture in defense paired with another unique feature: their spatulate sting applies venom topically instead of piercing the skin of the attacker (Marlier et al. 2004). Unfortunately, while hypotheses of diversification associated with dispersal and ecological opportunity could be tested with extended species-level phylogenetic and biological data, hypotheses regarding the evolutionary significance and influence of innovative features are difficult to test and must remain somewhat speculative.

In summary, we here present an improved genus-level phylogeny for the tribe Crematogastrini that provides the basis for recognizing 10 genus-group lineages. Our estimates show that these lineages have evolved over a relatively short time frame (50–70 Ma) from a Paleotropical ancestor. The position of the monotypic enigmatic Indomalayan genus *Rostromyrmex* as the sister lineage to all remaining lineages within the tribe prevents us from pinpointing a specific biogeographic region that acted as the cradle for the diversification of the tribe. However, we have strong support for an early diversification of Crematogastrini in the Afrotropical region within the *Cardiocondyla* and *Carebara* genus-groups, and then for a shift in emphasis toward the Indomalayan region as the center for crematogastrine diversification. We discerned several shifts in diversification rates related to the evolution of large, widespread genera, but were not able to associate these definitively with key evolutionary events such as dispersal or novel morphological characteristics. Arboreal habitats have been successfully colonized by only a few clades within Crematogastrini, but it appears that members of the tribe have remained faithful to their lofty nest sites once they adapted to utilize this habitat. Our genus-level study sets the scene for more detailed investigations of diversification and evolution in the delineated genus-group lineages using species-level phylogenies and biological data.

Data Availability Statement

Data from this study are available from the Dryad Digital Repository: doi:10.5061/dryad.121b453 (Blaimer et al. 2018).

Supplementary Data

Supplementary data are available at *Insect Systematics and Diversity* online.

Acknowledgments

We thank Eugenia Okonski for collection-based support at the Smithsonian Institution and Michele Esposito for support with AntWeb data uploads at the California Academy of Sciences. Stefan Cover graciously helped with loans from MCZC. We thank the following individuals for contributing specimens to this study: Himender Bharti, Marek Borowiec, Michael Branstetter, Chris Burwell, Katsuyuki Eguchi, Georg Fischer, David General, Yoshiaki Hashimoto, Peter Hawkes, Jürgen Heinze, Shingo Hoshoishi, Milan Janda, John Longino, Andrea Lucky, Florian Menzel, Dirk Mezger, Eli Sarnat, Robert Taylor, Alberto Tinaut, and Darren Ward. We further thank Michael Lloyd for assistance in laboratory methods and acknowledge general support for molecular work from L.A.B. staff. All of the laboratory work was conducted in and with the support of the L.A.B. facilities of the National Museum of Natural History. Phylogenomic analyses utilized the Smithsonian Institution High Performance Cluster (SI/HPC). This research was supported by the National Science Foundation (grants DEB-1555905 to S.G.B., DEB-1456964 to T.R.S., DEB-0842204 to P.S.W., and DEB-0842395 to B.L.F.). B.B.B. was supported by the USDA National Institute of Food and Agriculture Hatch project 1015782 during the analyses and writing stages of this work.

References Cited

Aleksandrova, G. N., and N. I. Zaporozhets. 2008. Palynological characteristics of Upper Cretaceous and Paleogene deposits on the west of the

Sambian Peninsula (Kaliningrad region), Part 2. Stratigr. Geol. Correl. 16: 528–539.

Anderson, K. E., T. A. Linksvayer, and C. R. Smith. 2008. The causes and consequences of genetic caste determination in ants (Hymenoptera: Formicidae). Myrmecol. News. 11: 119–132.

AntCat. 2018. An online catalog of the ants of the world. http://www.antcat.org/

Archibald, S. B., D. R. Greenwood, and R. W. Mathewes. 2013. Seasonality, montane beta diversity, and Eocene insects: testing Janzen's dispersal hypothesis in an equable world. Palaeogeogr. Palaeoclimatol. Palaeoecol. 371: 1–8.

Bayzid, M. S., S. Mirarab, B. Boussau, and T. Warnow. 2015. Weighted statistical binning: enabling statistically consistent genome-scale phylogenetic analyses. PLoS One. 10: e0129183.

Blaimer, B. B. 2012. Acrobat ants go global–origin, evolution and systematics of the genus *Crematogaster* (Hymenoptera: Formicidae). Mol. Phylogenet. Evol. 65: 421–436.

Blaimer, B. B., S. G. Brady, T. R. Schultz, M. W. Lloyd, B. L. Fisher, and P. S. Ward. 2015. Phylogenomic methods outperform traditional multi-locus approaches in resolving deep evolutionary history: a case study of formicine ants. BMC Evol. Biol. 15: 271.

Blaimer, B. B., M. W. Lloyd, W. X. Guillory, and S. G. Brady. 2016a. Sequence capture and phylogenetic utility of genomic ultraconserved elements obtained from pinned insect specimens. PLoS One. 11: e0161531.

Blaimer, B. B., J. S. LaPolla, M. G. Branstetter, M. W. Lloyd, and S. G. Brady. 2016b. Phylogenomics, biogeography and diversification of obligate mealybug-tending ants in the genus *Acropyga*. Mol. Phylogenet. Evol. 102: 20–29.

Blaimer, B. B., P. S. Ward, T. R. Schultz, B. L. Fisher, and S. G. Brady. 2018. Data from: Paleotropical diversification dominates the evolution of the hyperdiverse ant tribe Crematogastrini (Hymenoptera: Formicidae). Dryad Digital Repository. doi:10.5061/dryad.121b453.

Blanchard, B. D., and C. S. Moreau. 2016. Defensive traits exhibit an evolutionary trade-off and drive diversification in ants. Evolution. 71: 315–328.

Blumenstiel, B., K. Cibulskis, S. Fisher, M. DeFelice, A. Barry, T. Fennell, J. Abreu, B. Minie, M. Costello, and G. Young. 2010. Targeted exon sequencing by in-solution hybrid selection. Curr. Protoc. Hum. Genet. Chapter 18: Unit 18.4.

Bolger, A. M., M. Lohse, and B. Usadel. 2014. Trimmomatic: a flexible trimmer for Illumina sequence data. Bioinformatics. 30: 2114–2120.

Borowiec, M. L. 2016. AMAS: a fast tool for alignment manipulation and computing of summary statistics. PeerJ. 4: e1660.

Borowiec, M. L., E. K. Lee, J. C. Chiu, and D. C. Plachetzki. 2015. Extracting phylogenetic signal and accounting for bias in whole-genome data sets supports the Ctenophora as sister to remaining Metazoa. BMC Genomics. 16: 987.

Bossert, S., E. A. Murray, B. B. Blaimer, and B. N. Danforth. 2017. The impact of GC bias on phylogenetic accuracy using targeted enrichment phylogenomic data. Mol. Phylogenet. Evol. 111: 149–157.

Bouckaert, R., J. Heled, D. Kühnert, T. Vaughan, C. H. Wu, D. Xie, M. A. Suchard, A. Rambaut, and A. J. Drummond. 2014. BEAST 2: a software platform for Bayesian evolutionary analysis. PLoS Comput. Biol. 10: e1003537.

Branstetter, M. G., J. T. Longino, P. S. Ward, and B. C. Faircloth. 2017a. Enriching the ant tree of life: enhanced UCE bait set for genome-scale phylogenetics of ants and other Hymenoptera. Methods Ecol. Evol. 8: 768–776.

Branstetter, M. G., A. Ješovnik, J. Sosa-Calvo, M. W. Lloyd, B. C. Faircloth, S. G. Brady, and T. R. Schultz. 2017b. Dry habitats were crucibles of domestication in the evolution of agriculture in ants. Proc. R. Soc. B. 284: 20170095.

Branstetter, M. G., B. N. Danforth, J. P. Pitts, B. C. Faircloth, P. S. Ward, M. L. Buffington, M. W. Gates, R. R. Kula, and S. G. Brady. 2017c. Phylogenomic insights into the evolution of stinging wasps and the origins of ants and bees. Curr. Biol. 27: 1019–1025.

Brown, W. L. 2000. Diversity of ants, pp. 45–79. *In* J. D. Majer, L. E. Alonso, and T. R. Schultz (eds.), Ants: standard methods for measuring and monitoring biodiversity. Smithsonian Institution Press, Washington, DC.

Brown, J. W., and S. A. Smith. 2017. The past sure is tense: on interpreting phylogenetic divergence time estimates. Syst. Biol. 67: 340–353.

Buren, W. F. 1959. A review of the species of *Crematogaster* sensu stricto, in North America (Hymenoptera: Formicidae), part I. J.N.Y. Entomol. Soc. 66: 119–134.

Buschinger, A. 2009. Social parasitism among ants: a review (Hymenoptera: Formicidae). Myrmecol. News. 12: 219–235.

Castresana, J. 2000. Selection of conserved blocks from multiple alignments for their use in phylogenetic analysis. Mol. Biol. Evol. 17: 540–552.

Cox, C. B. 2001. The biogeographic regions reconsidered. J. Biogeogr. 28: 511–523.

Dunn, C. W., G. Giribet, G. D. Edgecombe, and A. Hejnol. 2014. Animal phylogeny and its evolutionary implications. Annu. Rev. Ecol. Evol. Syst. 45: 371–395.

Faircloth, B. 2013. Illumiprocessor: a trimmomatic wrapper for parallel adapter and quality trimming. http://dx.doi.org/10.6079/J6079ILL

Faircloth, B. C. 2016. PHYLUCE is a software package for the analysis of conserved genomic loci. Bioinformatics. 32: 786–788.

Faircloth, B. C., and T. C. Glenn. 2012. Not all sequence tags are created equal: designing and validating sequence identification tags robust to indels. PLoS One. 7: e42543.

Faircloth, B. C., J. E. McCormack, N. G. Crawford, M. G. Harvey, R. T. Brumfield, and T. C. Glenn. 2012. Ultraconserved elements anchor thousands of genetic markers spanning multiple evolutionary timescales. Syst. Biol. 61: 717–726.

Faircloth, B. C., M. G. Branstetter, N. D. White, and S. G. Brady. 2015. Target enrichment of ultraconserved elements from arthropods provides a genomic perspective on relationships among Hymenoptera. Mol. Ecol. Resour. 15: 489–501.

Fisher, S., A. Barry, J. Abreu, B. Minie, J. Nolan, T. M. Delorey, G. Young, T. J. Fennell, A. Allen, and L. Ambrogio. 2011. A scalable, fully automated process for construction of sequence-ready human exome targeted capture libraries. Genome Biol. 12: R1.

Frandsen, P. B., B. Calcott, C. Mayer, and R. Lanfear. 2015. Automatic selection of partitioning schemes for phylogenetic analyses using iterative k-means clustering of site rates. BMC Evol. Biol. 15: 13.

Gauld, I. D., and B. Bolton. 1988. The Hymenoptera. Oxford University Press, Oxford, United Kingdom.

Grabherr, M. G., B. J. Haas, M. Yassour, J. Z. Levin, D. A. Thompson, I. Amit, X. Adiconis, L. Fan, R. Raychowdhury, Q. Zeng, et al. 2011. Full-length transcriptome assembly from RNA-Seq data without a reference genome. Nat. Biotechnol. 29: 644–652.

Hölldobler, B., M. Obermayer, N. J. Plowes, and B. L. Fisher. 2014. New exocrine glands in ants: the hypostomal gland and basitarsal gland in the genus *Melissotarsus* (Hymenoptera: Formicidae). Naturwissenschaften. 101: 527–532.

Jarvis, E. D., S. Mirarab, A. J. Aberer, B. Li, P. Houde, C. Li, S. Y. Ho, B. C. Faircloth, B. Nabholz, and J. T. Howard. 2014. Whole-genome analyses resolve early branches in the tree of life of modern birds. Science. 346: 1320–1331.

Ješovnik, A., J. Sosa-Calvo, M. W. Lloyd, M. G. Branstetter, F. Fernandez, and T. R. Schultz. 2017. Phylogenomic species delimitation and host-symbiont coevolution in the fungus-farming ant genus *Sericomyrmex* Mayr (Hymenoptera: Formicidae): ultraconserved elements (UCEs) resolve a recent radiation. Syst. Ent. 42: 523–542.

Katoh, K., G. Asimenos, and H. Toh. 2009. Multiple alignment of DNA sequences with MAFFT, pp. 39–64. *In* D. Posada (ed.), Bioinformatics for DNA sequence analysis. Springer, New York, NY.

Kugler, C. 1979. Evolution of the sting apparatus in the myrmicine ants. Evolution. 33: 117–130.

Lach, L., C. Parr, and K. Abbott. 2010. Ant ecology. Oxford University Press, Oxford, United Kingdom.

Lanfear, R., P. B. Frandsen, A. M. Wright, T. Senfeld, and B. Calcott. 2017. PartitionFinder 2: new methods for selecting partitioned models of evolution for molecular and morphological phylogenetic analyses. Mol. Biol. Evol. 34: 772–773.

LaPolla, J. S., G. M. Dlussky, and V. Perrichot. 2013. Ants and the fossil record. Annu. Rev. Entomol. 58: 609–630.

Lemmon, E. M., and A. R. Lemmon. 2013. High-throughput genomic data in systematics and phylogenetics. Annu. Rev. Ecol. Evol. Syst. 44: 99–121.

Lucky, A., and E. M. Sarnat. 2010. Biogeography and diversification of the Pacific ant genus *Lordomyrma* Emery. J. Biogeogr. 37: 624–634.

Lucky, A., M. D. Trautwein, B. S. Guénard, M. D. Weiser, and R. R. Dunn. 2013. Tracing the rise of ants - out of the ground. PLoS One. 8: e84012.

Marlier, J. F., Y. Quinet, and J. C. de Biseau. 2004. Defensive behaviour and biological activities of the abdominal secretion in the ant *Crematogaster scutellaris* (Hymenoptera: Myrmicinae). Behav. Processes. 67: 427–440.

Matzke, N. J. 2013. Probabilistic historical biogeography: new models for founder-event speciation, imperfect detection, and fossils allow improved accuracy and model-testing. University of California, Berkeley, CA.

Matzke, N. J. 2014. Model selection in historical biogeography reveals that founder-event speciation is a crucial process in Island Clades. Syst. Biol. 63: 951–970.

Meyer, A. L. S., and J. J. Wiens. 2018. Estimating diversification rates for higher taxa: BAMM can give problematic estimates of rates and rate shifts. Evolution. 72: 39–53.

Mirarab, S., and T. Warnow. 2015. ASTRAL-II: coalescent-based species tree estimation with many hundreds of taxa and thousands of genes. Bioinformatics. 31: i44–i52.

Mirarab, S., R. Reaz, M. S. Bayzid, T. Zimmermann, M. S. Swenson, and T. Warnow. 2014. ASTRAL: genome-scale coalescent-based species tree estimation. Bioinformatics. 30: i541–i548.

Misof, B., S. Liu, K. Meusemann, R. S. Peters, A. Donath, C. Mayer, P. B. Frandsen, J. Ware, T. Flouri, R. G. Beutel, et al. 2014. Phylogenomics resolves the timing and pattern of insect evolution. Science. 346: 763–767.

Moore, B. R., S. Höhna, M. R. May, B. Rannala, and J. P. Huelsenbeck. 2016. Critically evaluating the theory and performance of Bayesian analysis of macroevolutionary mixtures. Proc. Natl. Acad. Sci. USA. 113: 9569–9574.

Perrichot, V., S. Lacau, D. Néraudeau, and A. Nel. 2007. Fossil evidence for the early ant evolution. Naturwissenschaften. 95: 85–90.

Prebus, M. 2017. Insights into the evolution, biogeography and natural history of the acorn ants, genus *Temnothorax* Mayr (hymenoptera: Formicidae). BMC Evol. Biol. 17: 250.

Price, S. L., S. Powell, D. J. Kronauer, L. A. Tran, N. E. Pierce, and R. K. Wayne. 2014. Renewed diversification is associated with new ecological opportunity in the Neotropical turtle ants. J. Evol. Biol. 27: 242–258.

Price, S. L., R. S. Etienne, and S. Powell. 2016. Tightly congruent bursts of lineage and phenotypic diversification identified in a continental ant radiation. Evolution. 70: 903–912.

Prum, R. O., J. S. Berv, A. Dornburg, D. J. Field, J. P. Townsend, E. M. Lemmon, and A. R. Lemmon. 2015. A comprehensive phylogeny of birds (Aves) using targeted next-generation DNA sequencing. Nature. 526: 569–573.

Rabosky, D. L. 2014. Automatic detection of key innovations, rate shifts, and diversity-dependence on phylogenetic trees. PLoS One. 9: e89543.

Rabosky, D. L., F. Santini, J. Eastman, S. A. Smith, B. Sidlauskas, J. Chang, and M. E. Alfaro. 2013. Rates of speciation and morphological evolution are correlated across the largest vertebrate radiation. Nat. Commun. 4: 1958.

Rabosky, D. L., M. Grundler, C. Anderson, J. J. Shi, J. W. Brown, H. Huang, and J. G. Larson. 2014. BAMMtools: an R package for the analysis of evolutionary dynamics on phylogenetic trees. Methods Ecol. Evol. 5: 701–707.

Rabosky, D. L., J. S. Mitchell, and J. Chang. 2017. Is BAMM flawed? Theoretical and practical concerns in the analysis of multi-rate diversification models. Syst. Biol. 66: 477–498.

Ree, R. H., and S. A. Smith. 2008. Maximum likelihood inference of geographic range evolution by dispersal, local extinction, and cladogenesis. Syst. Biol. 57: 4–14.

Rohland, N., and D. Reich. 2012. Cost-effective, high-throughput DNA sequencing libraries for multiplexed target capture. Genome Res. 22: 939–946.

Stamatakis, A. 2014. RAxML version 8: a tool for phylogenetic analysis and post-analysis of large phylogenies. Bioinformatics. 30: 1312–1313.

Tagliacollo, V. A., and R. Lanfear. 2018. Estimating improved partitioning schemes for ultraconserved elements. Mol. Biol. Evol. 35: 1798–1811.

Tank, D. C., J. M. Eastman, M. W. Pennell, P. S. Soltis, D. E. Soltis, C. E. Hinchliff, J. W. Brown, E. B. Sessa, and L. J. Harmon. 2015. Nested radiations and the pulse of angiosperm diversification: increased diversification rates often follow whole genome duplications. New Phytol. 207: 454–467.

Toussaint, E. F., L. Hendrich, H. Shaverdo, and M. Balke. 2015. Mosaic patterns of diversification dynamics following the colonization of Melanesian islands. Sci. Rep. 5: 16016.

Ward, P. S. 2014. The phylogeny and evolution of ants. Annu. Rev. Ecol. Evol. Syst. 45: 23–43.

Ward, P. S., and M. G. Branstetter. 2017. The acacia ants revisited: convergent evolution and biogeographic context in an iconic ant/plant mutualism. Proc. R. Soc. London, Ser. B. 284: 20162569.

Ward, P. S., S. G. Brady, B. L. Fisher, and T. R. Schultz. 2015. The evolution of myrmicine ants: phylogeny and biogeography of a hyperdiverse ant clade (Hymenoptera: Formicidae). Syst. Ent. 40: 61–81.

Wilson, E. O., and B. Hölldobler. 1990. The ants. Harvard University Press, Cambridge, MA.

Wilson, E. O., and B. Hölldobler. 2005. The rise of the ants: a phylogenetic and ecological explanation. Proc. Natl. Acad. Sci. USA. 102: 7411–7414.

Zachos, J., M. Pagani, L. Sloan, E. Thomas, and K. Billups. 2001. Trends, rhythms, and aberrations in global climate 65 Ma to present. Science. 292: 686–693.

Zachos, J. C., G. R. Dickens, and R. E. Zeebe. 2008. An early Cenozoic perspective on greenhouse warming and carbon-cycle dynamics. Nature. 451: 27.